

## **A multi-channel based illumination compensation mechanism for brightness invariant image retrieval**

**Shiv Ram Dubey · Satish Kumar Singh · Rajat Kumar Singh**

This paper has been published by Multimedia Tools and Applications, Springer.

The final publication is available at <http://link.springer.com/article/10.1007/s11042-014-2226-5>.

Please cite this paper as “Shiv Ram Dubey, Satish Kumar Singh, Rajat Kumar Singh, "A multi-channel based illumination compensation mechanism for brightness invariant image retrieval," *Multimedia Tools and Applications*, vol. 74, no. 24, pp. 11223-11253, 2015.”

**Abstract** The image retrieval is still challenging to retrieve the most similar images of a given image from a huge database more accurately and robustly. It becomes more challenging for the images having drastic illumination differences. Most of feature descriptor having better retrieval performance degrades in the case of illumination change. To circumvent this problem, we compensated the varying illumination in the image using multi-channel information. We used red, green, blue channel of RGB color space and I channel of HSI color space to remove the intensity change in the image. Finally, we designed an illumination compensated color space to compute the feature descriptor over it. The proposed idea is generic and can be implemented with the most of the feature descriptor. We used some state-of-the-art feature descriptor to show the effectiveness and robustness of proposed color transformation towards uniform and non-uniform illumination change. The experimental results suggest that proposed brightness invariant color transformation can be applied effectively in the retrieval task.

**Keywords** Feature description · Complex illumination · Image retrieval · Brightness compensation

---

S. R. Dubey  
Indian Institute of Information Technology Allahabad,  
Devghat, Jhalwa, Allahabad, Uttar Pradesh, India  
e-mail: shivram1987@gmail.com

S. K. Singh  
Indian Institute of Information Technology Allahabad,  
Devghat, Jhalwa, Allahabad, Uttar Pradesh, India  
e-mail: sk.singh@iiita.ac.in

R. K. Singh  
Indian Institute of Information Technology Allahabad,  
Devghat, Jhalwa, Allahabad, Uttar Pradesh, India  
e-mail: rajatsingh@iiita.ac.in

## 1 Introduction

Over the years, numerous amounts of multimedia contents are being uploaded over the internet in the form of images, audios, videos, etc. It is still a very challenging task to index and retrieve images from the huge databases on the basis of the content of a query image. Illumination robust image matching and retrieval has been the bottleneck from the last two decades. In the published literature various approaches have been introduced to tackle the image retrieval problem [5, 16, 31, 42, 43]. Most of the description is based on the low-level features such as color, texture, shape, sketch etc. Color is a very important visual cue to differentiate between the two images. Color is widely used low-level feature in CBIR systems because of its simplicity and invariance. Scale and rotation invariance property of color histograms boost this feature for image retrieval and classification. Simplest color encoding is the global color histogram (GCH) which represents the frequency of each color in the image [9]. Some other color based feature descriptions are Color Coherence Vector (CCV) [21], and Color difference histogram (CDH) [17]. CCV encodes the color information into connected regions whereas CDH represents the image using color difference of two pixels in the image for each color and edge orientation. Recently, color information is also encoded in the form of histogram over the local feature regions (LFRs) extracted using Multi-scale Harris-Laplace detector [40]. Texture feature is important visual information of the image and widely adopted to represent the images. Local binary pattern (LBP) is most popular texture feature and it is widely used in many applications [18]. LBP is constructed by comparing the each pixel in the image with its neighboring pixels and according to the sign of comparison the LBP is generated. Recently, square symmetric local binary pattern (SSLBP) is introduced by Shi et al. [30] which is a variant of LBP. Some other LBP modifications are Centre symmetric local binary pattern (CS-LBP) [13], Local ternary pattern (LTP) [34], complete local binary pattern (CLBP) [10, 6] and local tetra patterns (LTrPs) [20]. Some texture features adopted for image retrieval are Border-interior pixel classification (BIC) [32] and Structure element histogram (SEH) [39]. Angular information is also used to represent the texture of the image [15, 27]. Color and texture features are integrated by Wang et al. for CBIR [41]. Shape and sketch based descriptors are also used to represent the features of the image in form of pattern and have shown attractive results for image retrieval [28, 26, 1]. A study of shape based retrieval techniques is done by Shahabi and Safar [28]. Saavedra and Bustos have applied the concept of local keyshapes as an alternative to the local keypoints to encode the shapes of the object for sketch-based image retrieval [26]. Shape retrieval is also incorporated in the sketch synthesis to obtain the information from both shape and sketch [1]. Shape and sketch based descriptors generally require edge detection and image segmentation which limits its applicability. Some other retrieval approaches are quadtree classified vector quantization [2], spatial relations [14], similarity refinement [29] and short and long term learning fusion [23]. Low-level feature descriptions represent the information in the image efficiently and used in several image matching problems but these features are sensitive to the illumination differences (i.e. photometric transformations) and fail to produce better result.

Some approaches also reported in the published literature to cope with the problem of illumination sensitivity. Illumination robust feature extraction transform (IRFET) is reported recently to detect the interest points in the image using contrast stretching functions (i.e. contrast signatures) [8]. In [38], bi-log transformation is used to remove the effect of the illumination variation but this approach needs to break the

intensity value into illumination and reflectance part which imposes extra computation and not always desirable. Some methods are also suggested for illumination robust face recognition [44, 3]. Logarithm Gradient Histogram (LGH) is proposed using spectral wavelength, magnitude and direction of the illumination for face recognition problem under varying illuminations [44]. In [3], illumination differences are compensated and normalized using discrete cosine transform (DCT) in the logarithm domain by truncating low-frequency DCT coefficients. However, this method requires a parameter tuning for the number of DCT coefficients to be truncated which differs in different illumination conditions. Texture is also represented by the Markov random field (MRF) [36] to achieve the spectrum invariance for CBIR systems. Ranganathan et al. [22] utilized probability distribution of descriptor space of training data to model the lighting changes in the feature description and to learn the system. To attain the anisotropic diffusion and to retain the gradient magnitude information, intensity level is multiplied with a large and constant weight (i.e. 2D image patches are embedded as 3D surfaces) which leads to a descriptor having invariance to intensity changes [19]. Order based approaches have been shown the promising image matching results under uniform illumination change [11, 12, 7, 35]. In [11], orders between certain pixels are used to penalize the difference between the patches. Only locally stable pixel pairs are chosen and order among each chosen pair is summarized to find the penalty required. Histogram of relative intensities (HRI) is used to encode the orders of pixels relative to the entire patch by Raj et al. [12]. They also proposed the Center-Symmetric Local Ternary Patterns (CSLTP) which is generalization of the CSLBP and combined it with the HRI to aggregate the complementary information. Local intensity order pattern (LIOP) is introduced which is intrinsically invariant to monotonic intensity change [7]. LIOP is constructed from the orders among the intensity values of the neighboring sample points of each pixel in the image. Tang et al. [35] introduced local OSID feature description from ordinal spatial distributions. OSID descriptor is obtained by grouping the pixel intensity values into both spatial and ordinal spaces. To encode the ordinal distribution information, they smoothed the intensities first in the patch to remove the noise with a Gaussian filter. After that, they sorted all the intensities and grouped into certain number of categories, where each category having the similar ordinal points. While these features perform well to match the images having uniform intensity change but they can't handle the complex or non-uniform illumination differences.

To overcome the drawbacks of the above mentioned descriptor, an illumination compensation algorithm is presented in this paper from multi-channel color intensity information. We transformed the RGB color space into a new illumination invariant  $R_{IC}G_{IC}B_{IC}$  color space by using red, green and blue components of RGB color and I component of HSI color. This new color space is generic in nature for the extraction of the feature descriptions of the images. The proposed multi-channel based illumination compensation mechanism is tested using color and texture features in image retrieval framework over three illumination datasets and found the appealing results. Experimental observations suggest that the introduced mechanism is robust to the illumination differences (i.e. for both uniform and non-uniform).

Rest of the paper is organized as follows: section 2 proposed a multi-channel based illumination compensation mechanism; section 3 introduces brightness invariant image retrieval; section 4 explores the similarity measures; section 5 presents the dataset, evaluation criteria and detailed result analysis over one natural and two synthesized illumination datasets; and finally section 6 concludes the article.

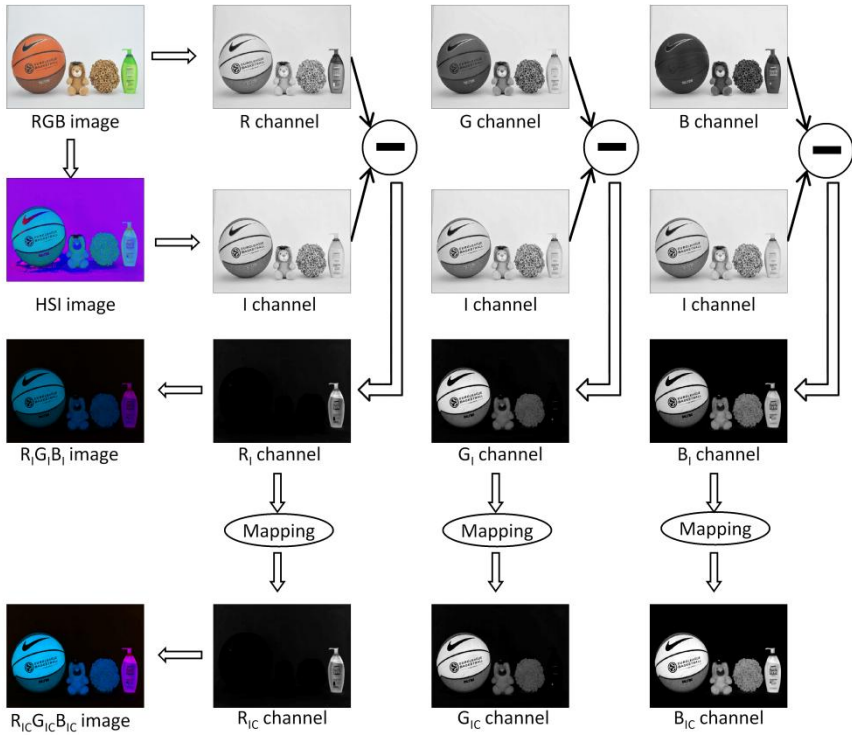


Fig. 1 Work flow of illumination compensation in  $R_{IC}G_{IC}B_{IC}$  color space

## 2 Illumination compensation

In this section, we introduce an approach to remove the effect of illumination difference in the color images. Color intensity compensation is performed using Red, Green, Blue and Intensity channels of the RGB and HSI color space of the image. By doing so, we generate a new color illumination compensated color space  $R_{IC}G_{IC}B_{IC}$ . The  $R_{IC}G_{IC}B_{IC}$  color space is composed of the three channels namely illumination compensated Red ( $R_{IC}$ ), illumination compensated Green ( $G_{IC}$ ) and illumination compensated Blue ( $B_{IC}$ ). The flowchart of the illumination compensation is illustrated in the Fig. 1. The mechanism operates in two phases (1) color intensity reduction and (2) contrast mapping.

### 2.1 Color Intensity Reduction

Color intensity reduction is the first step of the illumination compensation to remove the effect of illumination from the image. We have the initial RGB image  $M$  as an input image to be processed for illumination compensation. First of all, this method extracts the Red ( $R$ ), Green ( $G$ ), Blue ( $B$ ) and Intensity ( $I$ ) channels of the RGB and HSI image. To extract  $I$  component, image is transformed into the HSI color space. The range of  $I$  is between 0 and 1, whereas the range of  $R$ ,  $G$  and  $B$  is between 0 and  $l - 1$ , where  $l$  is the number of shade in each channel. To make the same range of each channel,  $R$ ,  $G$ , and  $B$  channels are normalized such that their ranges fall between 0 and 1. The normalization is performed by dividing each value of  $R$ ,  $G$ , and  $B$

components by  $l - 1$ . To compensate the illumination, the intensity  $I$  is subtracted from the  $R$ ,  $G$  and  $B$  channels. Let  $f_R(x, y)$ ,  $f_G(x, y)$  and  $f_B(x, y)$  be the functions to represent the normalized  $R$ ,  $G$  and  $B$  components of the image  $M$  where  $x$  and  $y$  are the rows and column of any pixel. We generated an illumination removed image  $M_I$  which consists of three components intensity reduced Red ( $R_I$ ), intensity reduced Green ( $G_I$ ) and intensity reduced Blue ( $B_I$ ).  $R_I$ ,  $G_I$  and  $B_I$  are obtained by reducing  $I$  component from  $R$ ,  $G$  and  $B$  components respectively as,

$$R_I = |f_R - I|, G_I = |f_G - I| \text{ and } B_I = |f_B - I| \quad (1)$$

where ‘ $| \cdot |$ ’ is the operator to find the absolute value. The  $I$  channel of HSI color can be derived from  $f_R, f_G$  and  $f_B$  as,

$$I = (f_R + f_G + f_B)/3 \quad (2)$$

From (1) and (2),  $R_I, G_I$  and  $B_I$  can be written as,

$$R_I = |(2f_R - f_G - f_B)/3|, G_I = |(2f_G - f_R - f_B)/3| \text{ and } B_I = |(2f_B - f_R - f_G)/3| \quad (3)$$

Let  $f_{R'}, f_{G'}$  and  $f_{B'}$  are the normalized Red, Green and Blue components of the image  $M'$  obtained after change in the illumination of image  $M$ . We represent  $f_{R'}, f_{G'}$  and  $f_{B'}$  of  $M'$  by following equations,

$$f_{R'} = f_R + e, f_{G'} = f_G + e \text{ and } f_{B'} = f_B + e \quad (4)$$

where  $e$  is the function of  $x$  and  $y$  to represent the difference in each channel caused by the change in the illumination. Note that difference  $e$  is also uniform for uniform intensity change and also non-uniform for non-uniform intensity change. In the case of uniform illumination change,  $e$  becomes a constant value. Conceptually, the range of  $e$  is  $-(l-1)$  to  $(l-1)$  where  $l$  is the number of shade in each channel of the image. The  $R'_I, G'_I$  and  $B'_I$  components of the illumination reduced  $M'_I$  using (3) is given as,

$$R'_I = |(2(f_R + e) - (f_G + e) - (f_B + e))/3|, G'_I = |(2(f_R + e) - (f_G + e) - (f_B + e))/3| \text{ and } B'_I = |(2(f_R + e) - (f_G + e) - (f_B + e))/3| \quad (5)$$

After simplify (5), we find,

$$R'_I = |(2f_R - f_G - f_B)/3|, G'_I = |(2f_G - f_R - f_B)/3| \text{ and } B'_I = |(2f_B - f_R - f_G)/3| \quad (6)$$

From (3) and (6), it is observed that,

$$R'_I = R_I, G'_I = G_I \text{ and } B'_I = B_I \quad (7)$$

Or we can say that,

$$M'_I = M_I \quad (8)$$

whereas, from (4), it can be pointed out that,

$$M' \neq M \text{ if } e \neq 0 \quad (9)$$

From (8) and (9), it is deduced that the images having illumination difference is not same but after color intensity reduction it becomes same (i.e. the effect of either uniform or non-uniform illumination is removed).

## 2.2 Contrast Mapping

It is observed that the range of each channel is reduced after color intensity subtraction phase. To map the range of each channel  $R_I, G_I$  and  $B_I$  back between 0 and  $l - 1$ , a contrast stretching strategy is adopted here. We refer the outputs of this step for  $R_I, G_I$  and  $B_I$  as illumination compensated Red ( $R_{IC}$ ), illumination compensated Green ( $G_{IC}$ ) and illumination compensated Blue ( $B_{IC}$ ). The mapping function used in this paper for contrast stretching is given as,

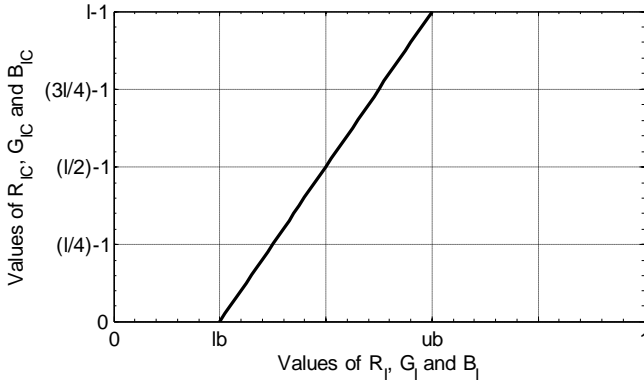


Fig. 2 Image retrieval using illumination compensation mechanism

$$R_{IC} = (R_i - lb) \times (l - 1)/(ub - lb), \quad G_{IC} = (G_i - lb) \times (l - 1)/(ub - lb)$$

$$\text{and } B_{IC} = (B_i - lb) \times (l - 1)/(ub - lb) \quad (10)$$

where  $lb$  and  $ub$  are the lower and upper bound for contrast stretching and given by,

$$lb = \min(lb_{R_i}, lb_{G_i}, lb_{B_i}) \quad (11)$$

$$ub = \max(ub_{R_i}, ub_{G_i}, ub_{B_i}) \quad (12)$$

where ‘ $\min$ ’ and ‘ $\max$ ’ are the operators to find the minimum and maximum values in a set of values respectively.  $lb_{R_i}$ ,  $lb_{G_i}$  and  $lb_{B_i}$  represents the bottom 1% of all pixel values of  $R_i$ ,  $G_i$  and  $B_i$  respectively.  $ub_{R_i}$ ,  $ub_{G_i}$  and  $ub_{B_i}$  represents the top 1% of all pixel values of  $R_i$ ,  $G_i$  and  $B_i$  respectively. This mapping function of contrast stretching is illustrated in the Fig. 2, where x-axis represents the old values before the mapping which is between  $lb$  and  $ub$  and y-axis represents the values obtained after the mapping. It should be noted that it is a linear function with  $lb$  and  $ub$  is mapped to the 0 and  $l - 1$  respectively, where  $l$  is number of shades in each channel after contrast stretching.

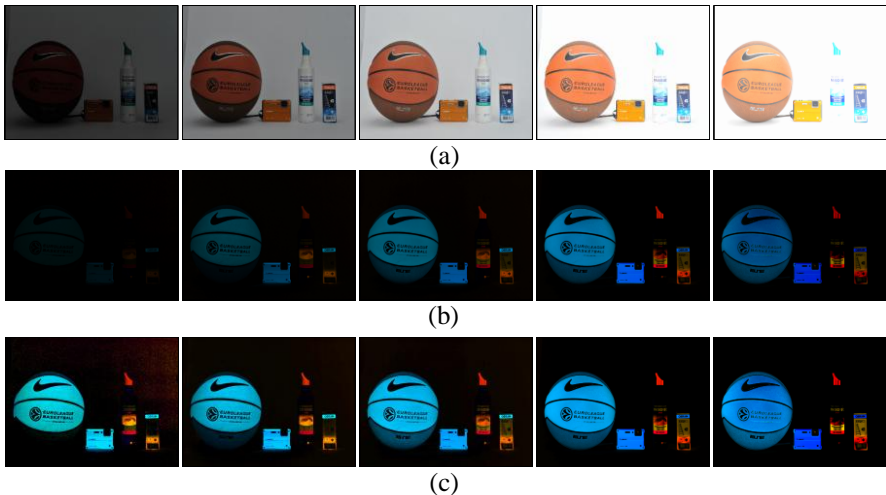


Fig. 3 Visualization of the illumination compensation steps (a) original images having uniform illumination differences, (b) intensity subtracted images, and (c) contrast stretched images.

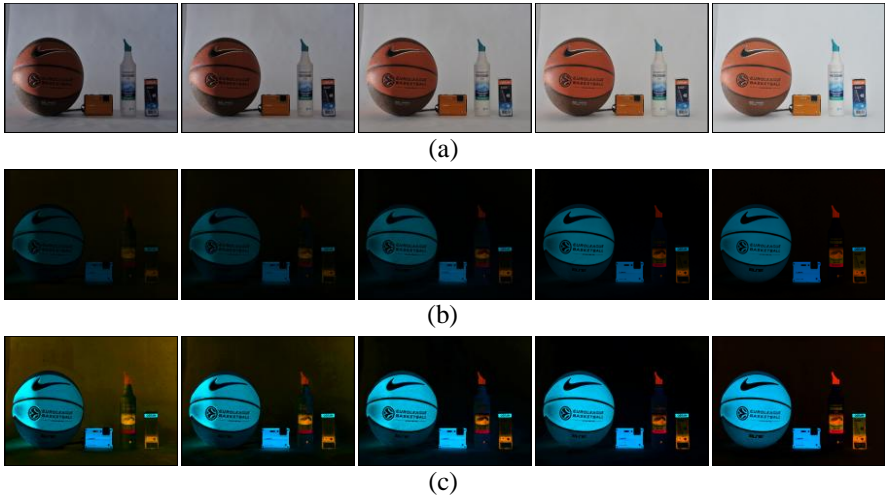


Fig. 4 Visualization of the illumination compensation steps (a) original images having non-uniform illumination differences, (b) intensity subtracted images, and (c) contrast stretched images.

The effect of intensity subtraction and contrast stretching can be visualized in the Fig. 3-4 for the images having illumination differences taken from the Phos illumination benchmark dataset. In Fig. 3, uniform illumination change is considered whereas non-uniform illumination difference is considered in Fig. 4. It can be easily observed that the images generated after the illumination compensation are having nearly same illumination irrespective of the amount of change in the illumination in their original images.

### 3 Brightness Invariant Retrieval

In this section, we describe the algorithm for image retrieval using illumination compensation which is inherently illumination invariant. Fig. 5 shows the steps involved to perform this task. The whole process consists of three steps (1) illumination compensation, (2) feature extraction, and (3) similarity measure and retrieval. Illumination compensation is the kind of pre-process as discussed in the previous section to remove the effect of illumination difference before the feature extraction.

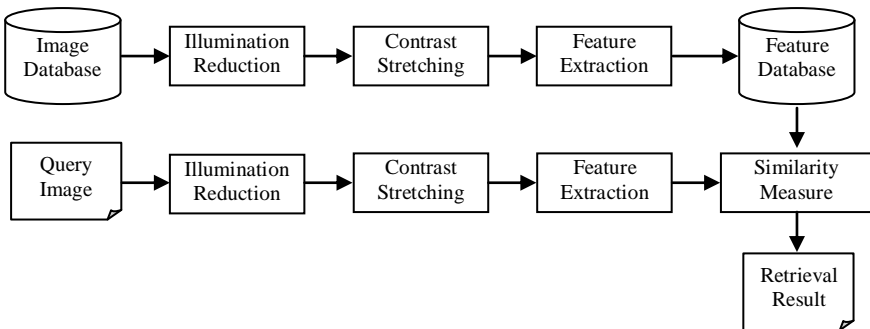


Fig. 5 Image retrieval using illumination compensation mechanism

In this paper, we extracted 6 different color or texture features namely Global Color Histogram (GCH) [9], Color Coherence Vector (CCV) [21], Border-Interior Classification (BIC) [32], Color Difference Histogram (CDH) [17], Structure Element Histogram (SEH) [39] and Square Symmetric Local Binary Pattern (SSLBP) [30] and performed the experiments with each feature individually. GCH, CCV and CDH are mainly the color based features whereas BIC, SEH and SSLBP are the texture based features. GCH is the simplest encoding of the color into histogram form whereas CCV computes the color histogram into coherent (i.e. connected) and incoherent regions. BIC is encoding of the feature on the basis of the pixel either lying over the boundary or inside. CDH is the representation of color difference of pixels situated at a certain distance and at a particular orientation. SEH finds the texture information of the image in the form of fine structures over each quantized color in HSV color space. SSLBP is the variant of LBP where square symmetric LBPs are considered as the same LBP. We refer GCH, CCV, BIC, CDH, SEH and SSLBP features extracted over illumination compensated image as  $GCH_{IC}$ ,  $CCV_{IC}$ ,  $BIC_{IC}$ ,  $CDH_{IC}$ ,  $SEH_{IC}$  and  $SSLBP_{IC}$  respectively in this paper. Whereas features extracted without illumination compensation is denoted by the GCH, CCV, BIC, CDH, SEH and SSLBP. The similarity measure used in this paper is discussed in the next section.

#### 4 Similarity Measure

We used proposed illumination compensation mechanism in content based image retrieval problem, where main goal is to find the most similar images of an image from a database of images. The similar images are extracted on the basis of the similarity score between the descriptor of query image and database images. If similarity score is less means images are more similar and vice-versa. We refer  $FD = \{fd_1, fd_2, \dots, fd_{dim}\}$  as the feature descriptor for the images in the database and  $TD = \{td_1, td_2, \dots, td_{dim}\}$  as the feature descriptor of the query image where  $dim$  is the dimension of the descriptor. Various performance measure matrices produce different similarity score for same set of image descriptors. In this paper, we use two distance measures used in SEH [39] and CDH [17] respectively. The distance metric used in [39] is defined as,

$$d_{SEH}(TD, FD) = \sum_{w=1}^{dim} \frac{|f_w - t_w|}{1 + f_w + t_w} \quad (13)$$

The distance metric used in [17] is defined as,

$$d_{CDH}(TD, FD) = \sum_{w=1}^{dim} \frac{|fd_w - td_w|}{|fd_w + f_{d_w}| + |td_w + t_{d_w}|} \quad (14)$$

where  $f_\mu = \sum_{w=1}^{dim} fd_w / dim$  and  $t_\mu = \sum_{w=1}^{dim} td_w / dim$ . We will compare the performances of features extracted with and without illumination compensation using these two distance measures in the experiments.

#### 5 Experiments and results

This section presents the result obtained by applying various descriptors with and without illumination compensation for image retrieval. We test the robustness of proposed illumination compensation mechanism under varying illumination condition. In this section, first we discuss about the illumination datasets which is



used in this paper for evaluation, and then we explore the evaluation criteria in detail, and finally present the experimental result with discussion.

## 5.1 Datasets

In order to evaluate the proposed descriptor, a standard Phos natural illumination database and two Corel synthesized illumination database is used in this paper for image retrieval. The Phos dataset consists of the 15 different categories with 15 images in each category having different degree of uniform and non-uniform illumination (9 images of uniform illumination and 6 images of non-uniform illumination). This dataset is obtained from <http://utopia.duth.gr/~dchrisos/pubs/database2.html>. Some sample images of Phos dataset is already shown in Fig. 1-3. We also synthesized two datasets Corel-uniform and Corel-non-uniform from the Corel-1000 dataset. Corel-1000 dataset is obtained from <http://wang.ist.psu.edu/~jwang/test1.tar>. Corel-1000 dataset contains 10 categories namely building, bus, dragon, elephant, flower, food, horse, human beings, landscapes and mountain. To synthesize the Corel-uniform dataset, we selected first 20 images of each category of Corel-1000 and generated 5 new images from each by adding  $-60, -30, 0, 30,$  and  $60$  in each channel of the original image. The number of images in each category of the Corel-uniform becomes 100 ( $20 \text{ image} \times 5 \text{ different intensity of uniform illumination}$ ). Fig. 6(a) shows the sample images from the Corel-uniform dataset. We also synthesized Corel-non-uniform from the same 20 images per category of the Corel-1000 dataset. 5 degree of different non-uniform illumination is adopted to generate 5 images of each original image including original one. Let  $im(x, y, t)$  be the color image of size  $u \times v$ , where the value of  $t$  is 1, 2, and 3 for red, green and blue components respectively and  $x$  and  $y$  are the rows and columns of any pixel. Then we generated five images  $im_w$  for  $w = -2, -1, 0, 1,$  and  $2$  from it as,

$$im_w(x, y, t) = im(x, y, t) - \left( w \times x \times \frac{30}{u} \right) - \left( w \times (v - y) \times \frac{30}{v} \right) - \left( w \times y \times \frac{20}{u} \right) - \left( w \times (v - x) \times \frac{20}{v} \right) \quad (15)$$

Now, Corel-non-uniform dataset is consists of the 10 categories with 100 images in each category ( $20 \text{ image} \times 5 \text{ different degree of non-uniform illumination}$ ). Fig. 6(b) shows the sample images from the Corel-non-uniform dataset.

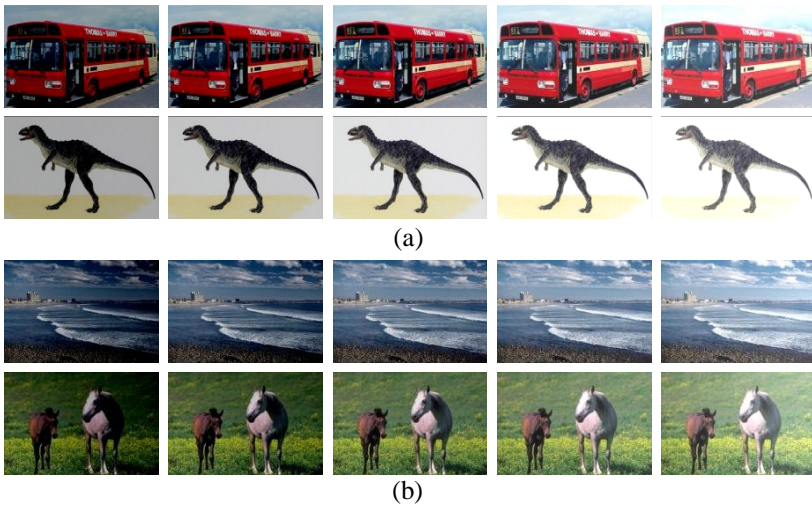


Fig. 6 Sample images from (a) Corel-uniform and (b) Corel-non-uniform dataset

## 5.2 Evaluation criteria

Most of the algorithms of image matching and image retrieval in the literature used *Precision* and *Recall* to measure the accuracy of the system. In content based image retrieval, the main task is to find most similar images of a query image in the whole database. We also adopted *Precision* and *Recall* curves to represent the effectiveness of proposed algorithm using different descriptors in image retrieval. Let there are total  $N_C$  number of category in the database and we retrieved  $r_1, r_2, \dots, r_e$  number of images (i.e. total  $e$  experiments having different number of retrieved images). Average precision rate (APR) and average recall rate (ARR) for the  $i$  number of retrieved images are given as,

$$APR(i) = \frac{\sum_{j=1}^{N_C} AP(i, j)}{N_C} \quad (16)$$

$$ARR(i) = \frac{\sum_{j=1}^{N_C} AR(i, j)}{N_C} \quad (17)$$

For  $j^{th}$  category, retrieval average precision (RAP) and retrieval average recall (RAR) are defined as,

$$RAP(j) = \frac{\sum_{i=r_1}^{r_e} AP(i, j)}{e} \quad (18)$$

$$RAR(j) = \frac{\sum_{i=r_1}^{r_e} AR(i, j)}{e} \quad (19)$$

Where,  $AP(i, j)$  and  $AR(i, j)$  are the average precision and average recall respectively for the  $j^{th}$  category when the  $i$  number of images are retrieved. We also measured the overall average precision (OAP) and overall average recall (OAR) as,

$$OAP = \frac{\sum_{j=1}^{N_C} RAP(j)}{N_C} \quad (20)$$

$$OAR = \frac{\sum_{j=1}^{N_C} RAR(j)}{N_C} \quad (21)$$

$AP(i, j)$  and  $AR(i, j)$  are calculated as,

$$AP(i, j) = \frac{\sum_{k=1}^{n_j} P_j(i, k)}{n_j} \quad (22)$$

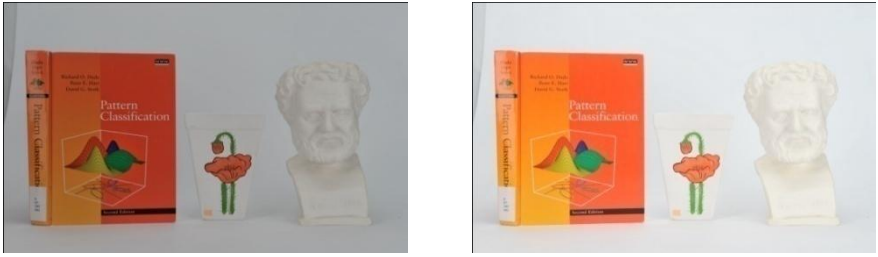
$$AR(i, j) = \frac{\sum_{k=1}^{n_j} R_j(i, k)}{n_j} \quad (23)$$

Where  $n_j$  is the number of images in the  $j^{th}$  category of that dataset,  $P_j(i, k)$  and  $R_j(i, k)$  are the precision and recall value when the  $i$  number of images are retrieved and  $k^{th}$  image of  $j^{th}$  category is considered as the query image.  $P_j(i, k)$  and  $R_j(i, k)$  are given as,

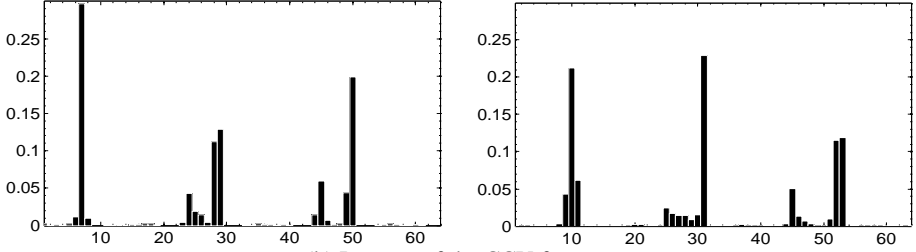
$$P_j(i, k) = \frac{NS}{i} \quad (24)$$

$$R_j(i, k) = \frac{NS}{ND} \quad (25)$$

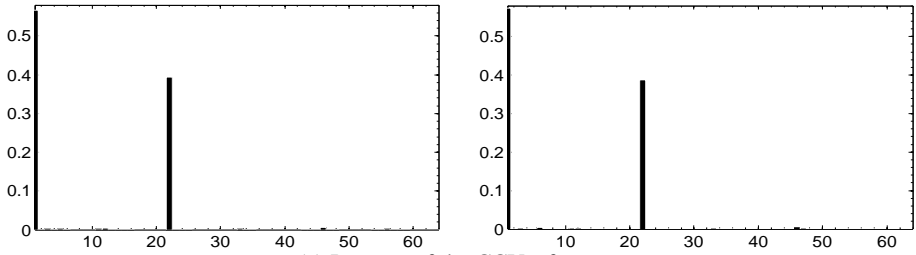
where  $NS$  is the number of similar images retrieved and  $ND$  is the number of similar images in the whole database. The value of  $i$  is considered from 5 to 15 in an interval of 1 for Phos dataset and it is from 5 to 40 in an interval of 5 for Corel-uniform and Corel-non-uniform datasets. The value of  $ND$  is 15 for the Phos database and 100 for Corel-uniform and Corel-non-uniform dataset.



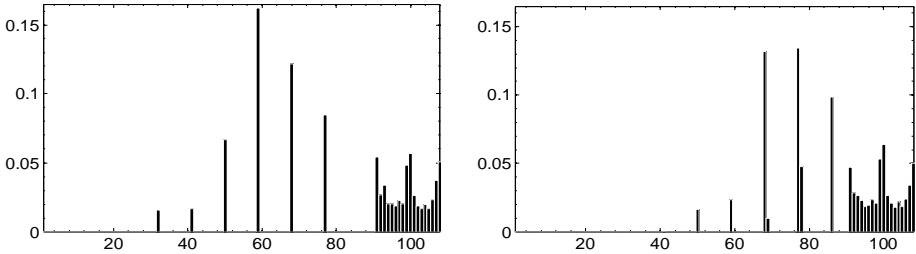
(a) Two images of Phos dataset having uniform illumination change



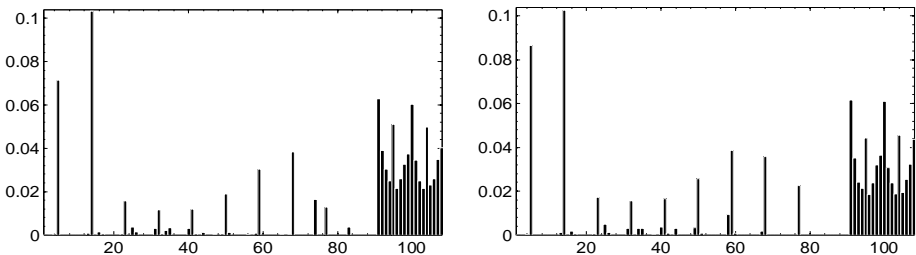
(b) Patterns of the CCV features



(c) Patterns of the CCV<sub>IC</sub> features



(d) Patterns of the CDH features

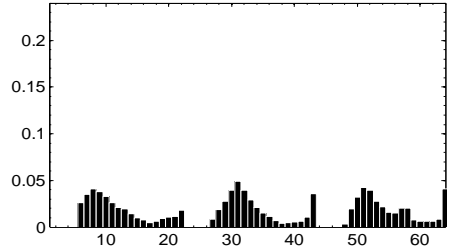
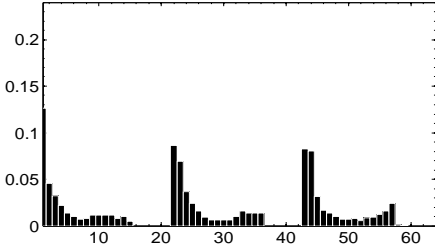


(e) Patterns of the CDH<sub>IC</sub> features

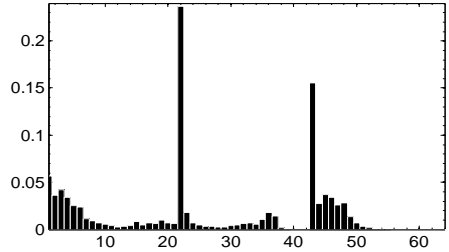
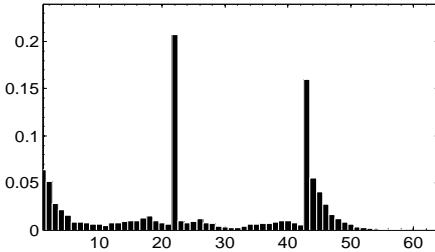
Fig. 7 Comparison between patterns extracted with and without illumination compensation using CCV and CDH features.



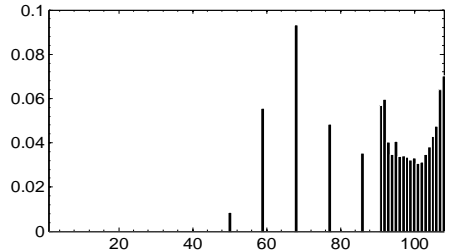
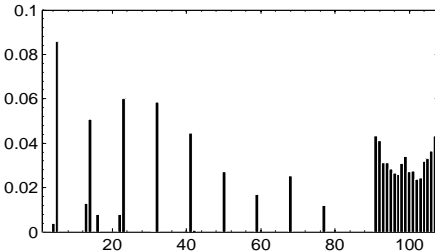
(a) Two images of Corel-uniform dataset having uniform illumination change



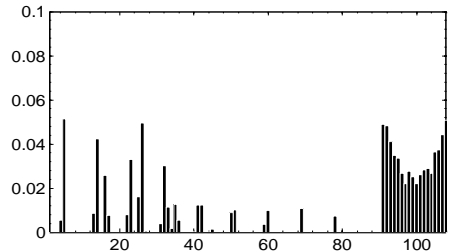
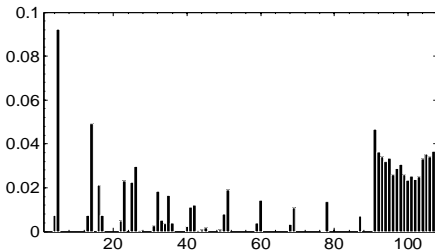
(B) Patterns of the GCH features



(c) Patterns of the  $GCH_{IC}$  features



(d) Patterns of the CDH features



(e) Patterns of the  $CDH_{IC}$  features

Fig. 8 Comparison between patterns extracted with and without illumination compensation using GCH and CDH features.

### 5.3 Experimental Results

Image retrieval is an application of image matching where a query image is matched with all images in a database and most appropriate similar images are returned on the basis of certain features. Matching two similar images having some geometric and photometric differences are still problematic. The main aim of our illumination compensation algorithm is to match the images under varying degree and intensity of uniform and non-uniform illumination. Fig. 7-9 represents the patterns extracted by different features with and without our approach for two images. The first column shows the first image and patterns for first image while second column shows the second image and patterns for second image using different features. We extracted CCV and CDH features with and without color intensity compensation over two images of Phos dataset in Fig.7 having uniform brightness change. It can be easily observed that the patterns of CCV (see Fig. 7(b)) and CDH (see Fig. 7(d)) are differing for both the images while it is nearly same for  $CCV_{IC}$  (see Fig. 7(c)) and  $CDH_{IC}$  (see Fig. 7(e)). In the case of CDH, even patterns are not fairly distributed which is obtained using  $CDH_{IC}$  as fairly distributed.

We also shown the patterns for GCH,  $GCH_{IC}$ , CDH and  $CDH_{IC}$  over a set of image having drastic uniform illumination change of Corel-uniform dataset in the Fig. 8. The patterns of  $GCH_{IC}$  and  $CDH_{IC}$  are more similar than the patterns of GCH and CDH respectively. Consider the case of the GCH (i.e. Fig. 8(b)), the most of the patterns at lower and higher bins are zero for either image while it is nonzero for other image, whereas it is very in the case of the patterns of the illumination compensated  $GCH_{IC}$  (i.e. Fig. 8(c)). Consider the case of CDH and  $CDH_{IC}$ , CDH patterns for images having complex brightness difference are also differs with large variation (i.e. fails to produce similar patterns) whereas it successfully overcome by  $CDH_{IC}$  (i.e. with brightness compensation) by producing similar patterns in such conditions.

To show the characteristics of proposed illumination compensation mechanism under non-uniform intensity change, we extracted the patterns using CCV,  $CCV_{IC}$ , BIC and  $BIC_{IC}$  for a set of image of Corel-non-uniform dataset in Fig. 9. For both the features CCV and BIC, patterns extracted with our approach are more similar than patterns extracted without intensity compensation. It should be noted that the patterns of CCV and BIC are distributed over each bin while it is not fully distributed in the patterns of the  $CCV_{IC}$  and  $BIC_{IC}$  but if any bin of the pattern using  $CCV_{IC}$  and  $BIC_{IC}$  is having zero value for one image then it is also nearly zero for the second value also (i.e. overall patterns are nearly equal using  $CCV_{IC}$  and  $BIC_{IC}$ ).

To test the degree of changes in the patterns extracted with and without brightness compensation, we considered two images of the Phos benchmark in Fig. 10 one is having very low illumination while another one is having very high illumination (see Fig. 10(a-b)). We calculated the difference among each corresponding bin of the patterns for both images extracted using GCH, CCV, BIC, CDH, SEH and SSLBP features with and without compensation. The feature with high amplitude at mean zero implies more number of bins having equal value in the patterns of both images while the curve near to mean represents the more number of bins in both patterns having less difference. We observed across the plots of Fig. 10 that each features combined with proposed approach has better similarities for both images as compared to standalone. CDH and SSLBP features make bigger difference when applied into the introduced system. From Fig. 7-10, it is deduced that proposed illumination compensation approach when combined with low-level image features boost the robustness of that feature.



(a) Two images of Corel-non-uniform dataset having non-uniform illumination change

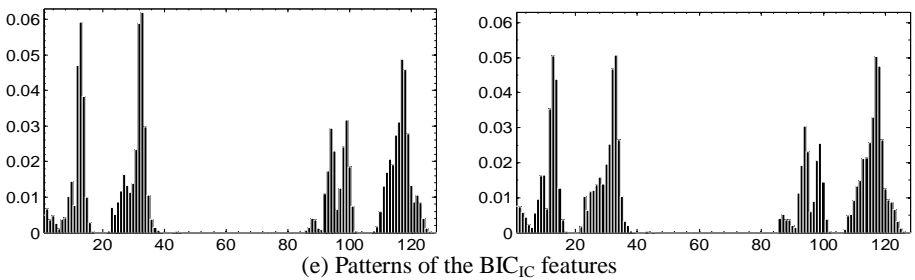
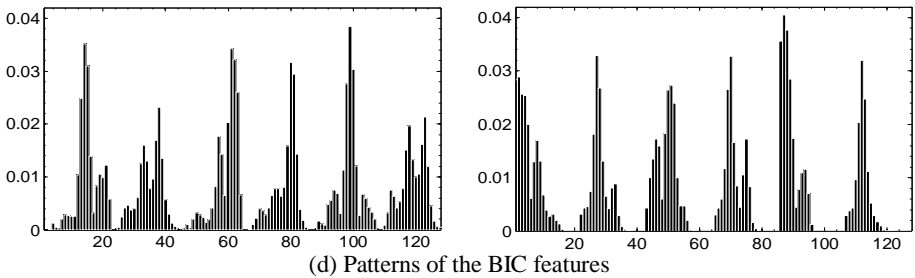
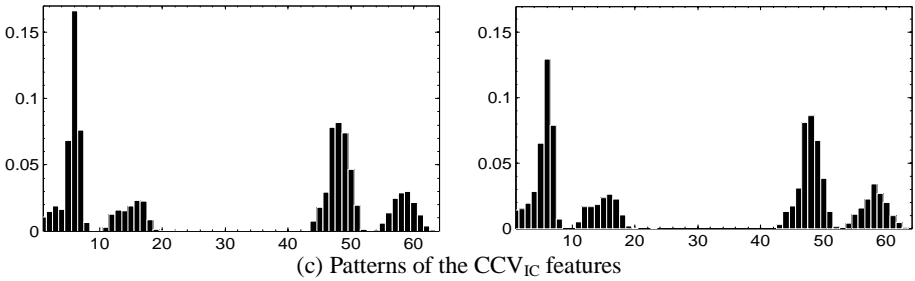
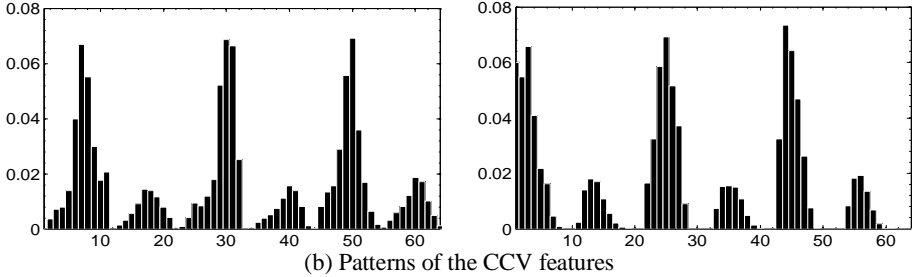


Fig. 9 Comparison between patterns extracted with and without illumination compensation using CCV and BIC features.

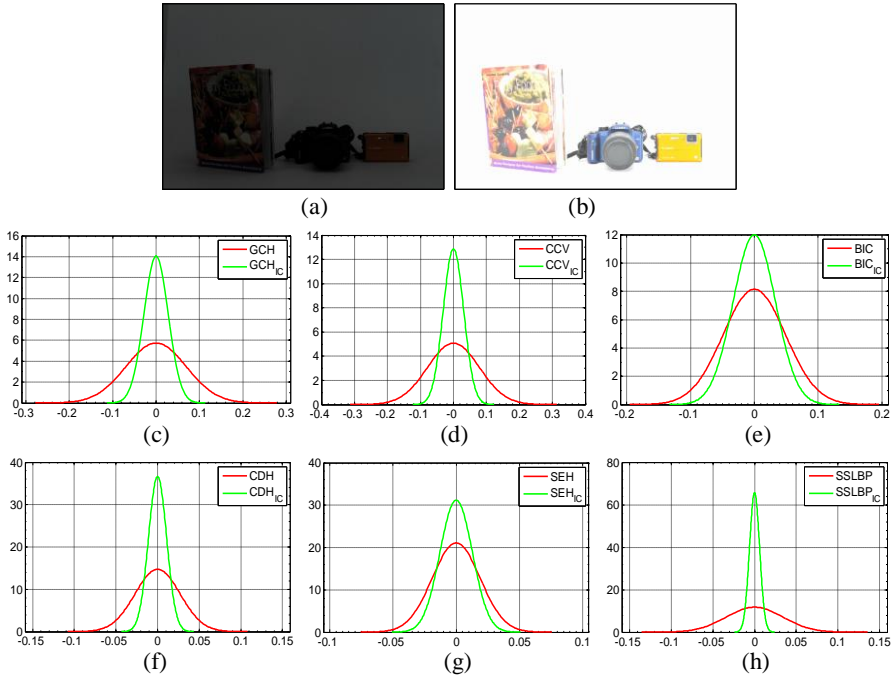


Fig. 10 Comparison between the normal distributions of the dissimilarities of patterns of two images at zero mean extracted with and without brightness compensation step.

### 5.3.1 Results on Phos dataset

We performed the image retrieval experiment over complete set of Phos illumination benchmark and precision-recall curves are presented in terms of average precision rate (APR) and average recall rate (ARR) in Fig. 11 using GCH, CCV, BIC, CDH, SEH and SSLBP features. We used two similarity measure  $d_{SEH}$  and  $d_{CDH}$  to test the effect of different distances over proposed compensation method. Both APR and ARR values are higher using both distances for each feature when images are preprocessed with proposed approach to remove the effect of illumination. It is understood that the degree of improvement in  $GCH_{IC}$ ,  $CCV_{IC}$ ,  $BIC_{IC}$  and  $CDH_{IC}$  are higher as compared to the  $SEH_{IC}$  and  $SSLBP_{IC}$ . The results of  $SSLBP_{IC}$  are not too improved but it is still better than the results of SSLBP.

To test the performance over each category of the dataset using each feature, we also find the retrieval average precision (RAP) and retrieval average recall (RAR) values as depicted in Table 1 and 2 respectively using  $d_{CDH}$  distance. All features when combined with proposed method are having more RAP and RAR values for most of the categories. The results which are improved are highlighted; the results in 4-5 categories using only  $SEH_{IC}$  and  $SSLBP_{IC}$  features are not improved but the overall improvement is found by these features as indicated by overall average precision (OAP) value in Table 1 and overall average recall (OAR) value in Table 2. OAP and OAR are improved in feature with illumination compensation step and amount of improvement is highest for the  $CDH_{IC}$  feature as compared to the CDH feature.

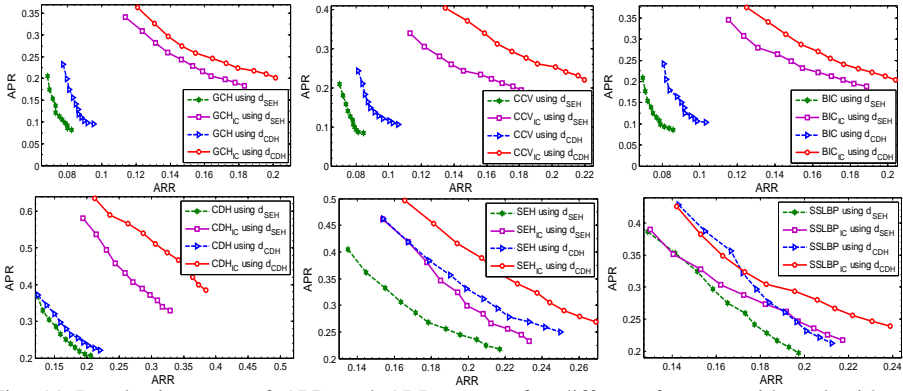


Fig. 11 Results in terms of APR and ARR curves for different features with and without illumination compensation using  $d_{SEH}$  and  $d_{CDH}$  similarity measures over Phos illumination benchmark dataset.

Table 1 RAP values for each category of Phos dataset using GCH,  $GCH_{IC}$ , CCV,  $CCV_{IC}$ , BIC,  $BIC_{IC}$ , CDH,  $CDH_{IC}$ , SEH,  $SEH_{IC}$ , SSLBP and  $SSLBP_{IC}$  features using  $d_{CDH}$  distance

Category	RAP using different features extracted from RGB and $R_{IC}G_{IC}B_{IC}$ color spaces											
	GCH	$GCH_{IC}$	CCV	$CCV_{IC}$	BIC	$BIC_{IC}$	CDH	$CDH_{IC}$	SEH	$SEH_{IC}$	SSLBP	$SSLBP_{IC}$
1	12.80	36.06	13.68	45.74	13.53	44.55	30.61	72.79	35.63	41.09	29.48	37.16
2	13.96	33.21	15.86	29.21	14.94	31.72	22.59	61.92	<b>34.99</b>	<b>26.75</b>	28.23	38.11
3	14.19	18.77	16.11	19.97	15.11	16.73	24.57	52.51	30.99	36.85	<b>39.09</b>	<b>34.83</b>
4	13.57	23.01	15.98	26.42	14.20	20.81	20.33	40.83	31.80	36.53	27.09	30.52
5	14.96	21.43	16.62	28.24	16.05	20.33	24.74	43.54	33.92	34.02	31.19	34.83
6	14.30	21.50	14.42	23.17	14.52	21.88	26.41	44.46	30.85	31.25	29.92	30.93
7	12.98	35.27	13.19	38.14	14.05	40.61	26.66	54.68	30.55	33.09	24.95	27.30
8	13.66	32.06	13.04	37.99	14.25	35.91	31.00	54.21	<b>31.13</b>	<b>31.04</b>	25.67	27.15
9	14.15	19.54	14.60	23.68	14.80	21.33	26.44	38.60	35.67	41.73	27.46	28.52
10	13.91	19.97	13.78	23.25	14.34	19.17	33.03	37.05	32.92	38.22	<b>29.12</b>	<b>27.58</b>
11	13.77	24.27	14.16	23.03	14.87	24.84	23.10	43.80	29.53	32.26	27.15	32.05
12	15.67	27.19	17.13	29.30	16.53	25.78	36.51	42.79	<b>30.67</b>	<b>30.55</b>	<b>32.18</b>	<b>29.07</b>
13	15.47	22.27	16.84	28.83	16.58	20.10	36.17	43.48	<b>34.03</b>	<b>29.56</b>	<b>31.48</b>	<b>24.97</b>
14	14.74	31.79	15.91	36.07	15.75	35.45	33.58	56.82	34.63	47.28	<b>31.10</b>	<b>28.06</b>
15	14.45	22.88	16.01	23.19	15.10	23.28	21.41	54.45	35.70	44.73	27.66	28.13
OAP	14.17	25.95	15.16	29.08	14.98	26.83	27.81	49.46	32.87	35.66	29.45	30.61

Table 2 RAR values for each category of Phos dataset using GCH,  $GCH_{IC}$ , CCV,  $CCV_{IC}$ , BIC,  $BIC_{IC}$ , CDH,  $CDH_{IC}$ , SEH,  $SEH_{IC}$ , SSLBP and  $SSLBP_{IC}$  features using  $d_{CDH}$  distance

Category	RAR using different features extracted from RGB and $R_{IC}G_{IC}B_{IC}$ color spaces											
	GCH	$GCH_{IC}$	CCV	$CCV_{IC}$	BIC	$BIC_{IC}$	CDH	$CDH_{IC}$	SEH	$SEH_{IC}$	SSLBP	$SSLBP_{IC}$
1	07.64	22.51	08.61	28.57	08.24	27.92	19.07	46.95	22.06	25.86	18.34	23.07
2	08.40	21.25	09.54	18.26	09.05	20.00	14.38	39.23	<b>21.78</b>	<b>16.73</b>	17.54	23.76
3	08.73	11.39	09.70	12.57	09.13	10.38	15.47	33.49	19.68	23.27	<b>23.84</b>	<b>22.06</b>
4	08.28	14.51	09.62	16.69	08.73	12.97	12.77	26.46	19.76	23.11	16.69	19.35
5	09.05	13.29	10.06	17.25	09.62	12.57	15.88	27.43	<b>20.81</b>	<b>20.77</b>	19.35	21.82
6	08.53	13.58	08.85	14.79	08.73	13.74	16.36	27.60	<b>19.23</b>	<b>18.99</b>	18.71	19.56
7	07.84	22.30	08.20	24.12	08.57	25.41	17.01	34.34	18.95	20.57	15.43	17.21
8	08.24	20.36	08.04	23.39	08.65	22.30	19.60	33.82	19.35	19.47	15.88	16.73
9	08.57	12.24	08.93	14.91	09.09	13.37	16.93	24.77	22.51	27.03	16.65	17.94
10	08.44	12.48	08.40	14.55	08.81	12.28	20.69	23.68	<b>20.48</b>	<b>23.88</b>	<b>17.90</b>	<b>17.21</b>
11	08.40	14.99	08.61	14.26	09.09	15.19	14.42	27.84	18.79	20.40	16.85	20.28
12	09.58	16.81	10.55	17.98	10.18	15.64	23.15	27.19	19.23	19.27	<b>20.12</b>	<b>18.42</b>
13	09.37	13.86	10.22	18.46	10.10	12.77	22.87	27.60	<b>21.66</b>	<b>18.02</b>	<b>19.68</b>	<b>15.47</b>
14	08.97	19.96	09.86	22.34	09.82	22.26	21.29	35.64	21.66	29.33	<b>19.43</b>	<b>18.30</b>
15	08.81	15.07	09.66	15.19	09.09	15.27	13.49	34.18	22.38	27.96	17.13	17.74
OAR	08.59	16.31	09.26	18.22	09.13	16.81	17.56	31.35	20.55	22.31	18.24	19.26



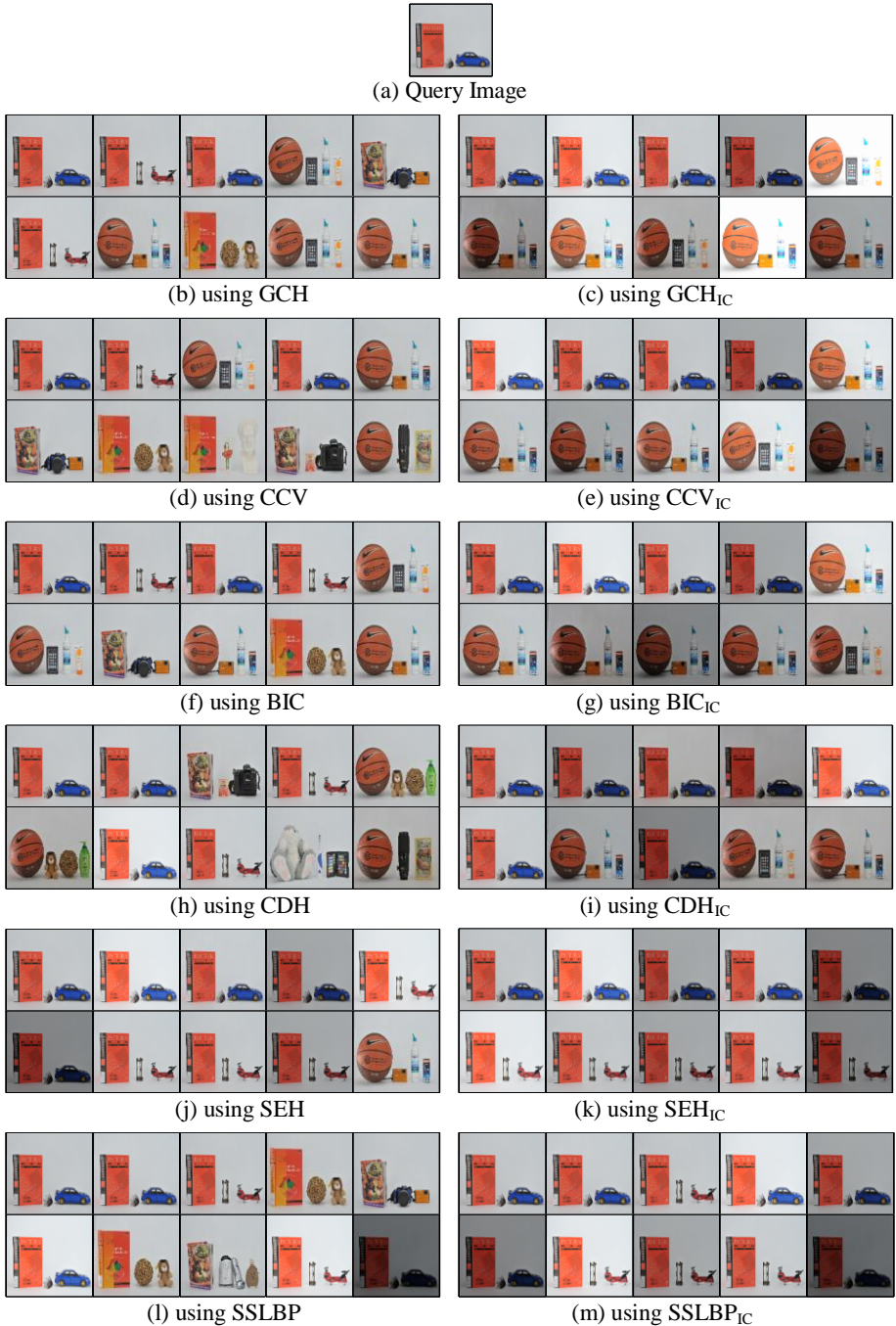


Fig. 12 Retrieval results using each feature to a query image of Phos dataset

To visualize the effect of proposed mechanism, top 10 retrieved images similar to a query image of Phos dataset are shown in Fig. 12 by each feature using  $d_{CDH}$  distance. GCH, CCV and BIC features are able to retrieve only two images of the same category (Fig. 12(b, d, f)) whereas  $GCH_{IC}$ ,  $CCV_{IC}$  and  $BIC_{IC}$  retrieved 4 similar

images each with 40% precision (Fig. 12(c, e, g)). Using CDH feature 3 similar images are returned whereas it is 7 using CDH<sub>IC</sub> feature (see Fig. 12 (h-i)). Using both SEH and SEH<sub>IC</sub>, 5 images are retrieved but the rank of returned images is better in the case of SEH<sub>IC</sub> (see Fig. 12(j-k)). It is observed that 6<sup>th</sup> image among returned images using SEH is similar to the query image and it should rank before the 5<sup>th</sup> image which is from the different category whereas it is successfully achieved using SEH<sub>IC</sub>. Using SSLBP and SSLBP<sub>IC</sub>, 4 and 6 similar images are found by the retrieval experiment as displayed in Fig. 12(l-m). Most number of similar images is retrieved by the CDH<sub>IC</sub> feature. From the retrieval results of Fig. 12, it is concluded that each feature retrieve more number of similar images having different brightness when it is operated after the illumination removal step proposed in this paper.

### 5.3.2 Results on Corel-uniform dataset

We also tested the discriminative ability of different features and the robustness of proposed method over Corel-uniform illumination synthesized dataset. The results are depicted in the Fig. 13 using APR and ARR values using both the similarity measures. An outstanding performance improvement is reported using CDH feature over uniform illumination. All features gained impressive positive result except SSLBP<sub>IC</sub> in this case but the result of SSLBP<sub>IC</sub> is still comparable. It can also be seen in Table 3 that the OAP and OAR values using GCH<sub>IC</sub>, CCV<sub>IC</sub>, BIC<sub>IC</sub> and CDH<sub>IC</sub> are better than GCH, CCV, BIC and CDH respectively using both distances. The overall results using SEH<sub>IC</sub> is better than SEH using only d<sub>CDH</sub> distance (see Table 3). This Table also reveals that SSLBP<sub>IC</sub> are not able to make an improvement over SSLBP in the uniform illumination case because it was improved in Table 1-2 (i.e. over Phos benchmark).

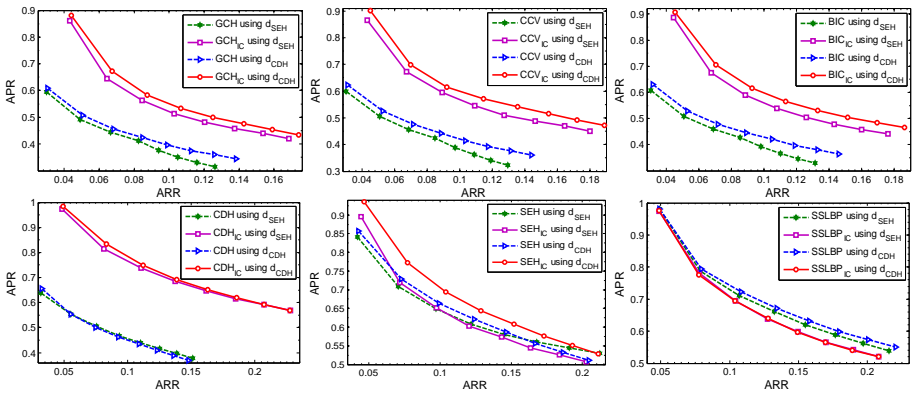


Fig. 13 Results in terms of APR and ARR curves for different features with and without illumination compensation using d<sub>SEH</sub> and d<sub>CDH</sub> similarity measures over Corel-uniform illumination synthesized dataset.

Table 3 OAP and OAR values for GCH, GCH<sub>IC</sub>, CCV, CCV<sub>IC</sub>, BIC, BIC<sub>IC</sub>, CDH, CDH<sub>IC</sub>, SEH, SEH<sub>IC</sub>, SSLBP and SSLBP<sub>IC</sub> features using d<sub>SEH</sub> and d<sub>CDH</sub> distance over Corel-uniform dataset

Mea- sure	Dist- ance	OAP and OAR using different features extracted from RGB and R <sub>IC</sub> G <sub>IC</sub> B <sub>IC</sub> color spaces											
		GCH	GCH <sub>IC</sub>	CCV	CCV <sub>IC</sub>	BIC	BIC <sub>IC</sub>	CDH	CDH <sub>IC</sub>	SEH	SEH <sub>IC</sub>	SSLBP	SSLBP <sub>IC</sub>
OAP	d <sub>SEH</sub>	41.43	54.80	42.48	57.43	42.94	57.12	47.45	70.44	<b>62.79</b>	<b>62.74</b>	<b>68.13</b>	<b>66.40</b>
	d <sub>CDH</sub>	43.40	56.72	45.10	60.08	45.56	59.76	47.22	71.10	63.21	66.34	<b>69.05</b>	<b>66.34</b>
OAR	d <sub>SEH</sub>	08.36	10.94	08.60	11.58	08.70	11.42	09.77	14.49	<b>13.10</b>	<b>12.86</b>	<b>13.88</b>	<b>13.44</b>
	d <sub>CDH</sub>	08.88	11.33	09.25	12.16	09.35	12.02	09.65	14.58	13.05	13.57	<b>14.12</b>	<b>13.43</b>

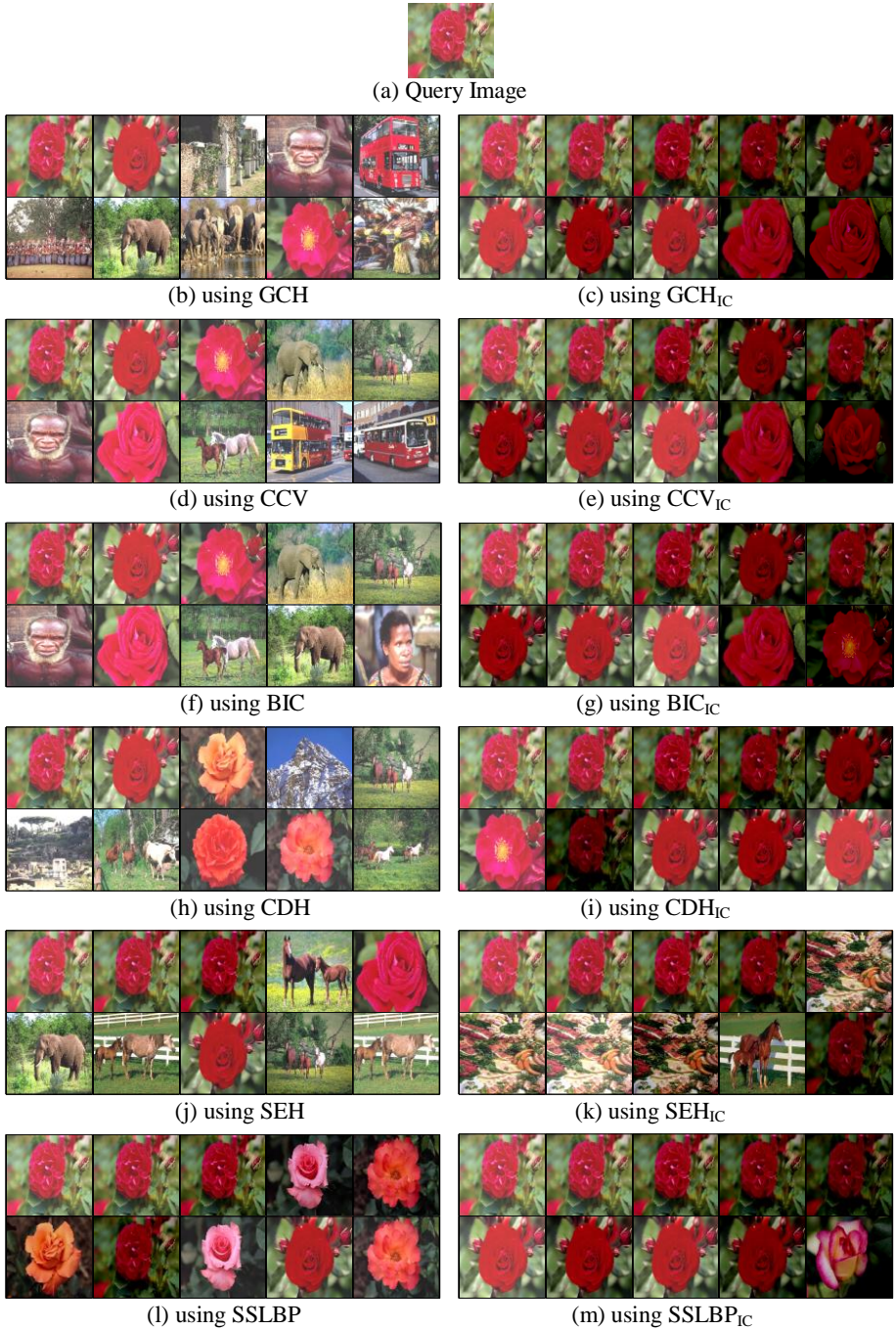


Fig. 14 Retrieval results using each feature from Corel-uniform dataset

We also retrieved the top 10 similar images to a query image of type flower to visualize the effect of introduced approach using  $d_{CDH}$  distance measure from Corel-uniform dataset (see Fig. 14). The query image is shown in Fig. 14(a). In the Corel-uniform dataset, there are 5 instances of the query image with varying brightness

whereas total 100 relevant images are present in the dataset. Using GCH feature, only three images are retrieved from the same category whereas using  $GCH_{IC}$  all 10 images returned are of the flower category (Fig. 14(b-c)). Another critical observation is the successfully retrieval of all 5 instances of the query image by  $GCH_{IC}$ . CCV and BIC features also failed to retrieve the all instances and using both only 4 images are retrieved from the same category (Fig. 14(d, f)), whereas  $CCV_{IC}$  and  $BIC_{IC}$  are able to retrieve all instances of the query image with 100% precision (Fig. 14(e, g)). CDH feature also fails to retrieve all instances and 5 similar images are retrieved by it with only 50% precision as depicted in Fig. 14(h) which is successfully overcome by  $CDH_{IC}$  by retrieving all instances with 100% retrieval precision as displayed in Fig. 14(i). Three instances of query image is returned by the retrieval system using SEH texture feature with 50% precision whereas  $SEH_{IC}$  retrieved all instances with 50% precision (see Fig. 14(j, k)). In this case the precision is same for both SEH and  $SEH_{IC}$  but using  $SEH_{IC}$  more semantically correct images are retrieved. The performance of SSLBP feature is good in this example, here using this feature system is able to gain 100% precision but only 4 instances are retrieved using this feature as shown in Fig. 14(l). The performance of SSLBP is good but its performance got boosted if it is generated after our illumination compensation preprocessing step (i.e.  $SSLBP_{IC}$ ) where 100% precision is earned with all instances of query image is also retrieved successfully (see Fig. 14(m)). It is deduced that the performance of each feature descriptor is enhanced in an attractive amount when applied with proposed retrieval system over the Corel-uniform dataset.

### 5.3.3 Results on Corel-non-uniform dataset

We also carried an experiment over Corel-non-uniform dataset using each feature derived with (i.e. in  $R_{IC}G_{IC}B_{IC}$  color space) and without (i.e. in RGB color space) illumination compensation. The results are demonstrated in the Fig. 15 for each feature using both distance measure. In this case also each feature in proposed  $R_{IC}G_{IC}B_{IC}$  color space performed outstanding with highest improvement in the  $CDH_{IC}$  feature. It should be noted that, the performance of  $SSLBP_{IC}$  was not better than SSLBP in uniform illumination case but it is reversed in this non-uniform illumination case (i.e. in this case  $SSLBP_{IC}$  is performing better than the SSLBP, see Fig. 15 and Table 4-5).

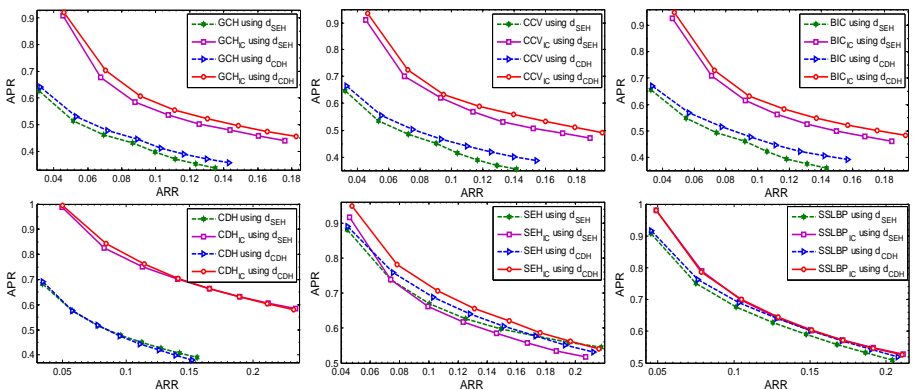


Fig. 15 APR and ARR results for different features with and without illumination compensation using  $d_{SEH}$  and  $d_{CDH}$  similarity measures over Corel-non-uniform synthesized dataset.

Table 4 RAP values for each category of Corel-non-uniform dataset using GCH, GCH<sub>IC</sub>, CCV, CCV<sub>IC</sub>, BIC, BIC<sub>IC</sub>, CDH, CDH<sub>IC</sub>, SEH, SEH<sub>IC</sub>, SSLBP and SSLBP<sub>IC</sub> features using d<sub>CDH</sub> distance

Features	RAP using d <sub>CDH</sub> over corel-nonuni for Image Category										OAP
	1	2	3	4	5	6	7	8	9	10	
GCH	25.43	29.47	<b>88.43</b>	29.02	45.89	28.72	55.78	52.11	30.13	26.50	41.15
GCH <sub>IC</sub>	53.26	62.75	<b>58.89</b>	39.58	74.46	40.58	75.38	43.11	43.15	43.67	53.48
CCV	25.02	36.59	<b>93.68</b>	33.42	57.27	25.42	55.31	<b>49.12</b>	32.19	29.71	43.77
CCV <sub>IC</sub>	56.28	68.98	<b>62.44</b>	39.55	79.19	41.78	77.37	<b>47.28</b>	44.03	48.79	56.57
BIC	26.59	33.84	<b>92.33</b>	35.40	57.20	26.50	57.94	52.45	31.97	30.45	44.47
BIC <sub>IC</sub>	55.14	67.31	<b>61.69</b>	40.69	77.91	42.91	77.71	43.72	43.36	50.27	56.07
CDH	38.43	67.33	64.41	37.84	45.45	27.03	37.23	48.76	29.64	44.35	44.05
CDH <sub>IC</sub>	60.79	85.00	70.53	53.59	83.47	44.98	79.99	67.17	46.76	67.89	66.02
SEH	54.44	63.98	<b>91.98</b>	46.10	<b>63.85</b>	<b>45.27</b>	82.86	58.15	40.98	<b>52.48</b>	60.01
SEH <sub>IC</sub>	65.41	69.86	<b>85.00</b>	50.28	<b>61.98</b>	<b>44.62</b>	83.04	61.57	42.56	<b>51.36</b>	61.57
SSLBP	51.98	76.81	<b>85.92</b>	48.72	<b>77.22</b>	<b>50.38</b>	64.17	58.63	36.34	44.01	59.42
SSLCP <sub>IC</sub>	56.85	81.36	<b>59.72</b>	47.36	<b>68.88</b>	<b>42.99</b>	83.13	66.30	40.52	61.63	60.88

Table 5 RAR values for each category of Corel-non-uniform dataset using GCH, GCH<sub>IC</sub>, CCV, CCV<sub>IC</sub>, BIC, BIC<sub>IC</sub>, CDH, CDH<sub>IC</sub>, SEH, SEH<sub>IC</sub>, SSLBP and SSLBP<sub>IC</sub> features using d<sub>CDH</sub> distance

Features	RAR using d <sub>CDH</sub> over corel-nonuni for Image Category										OAR
	1	2	3	4	5	6	7	8	9	10	
GCH	07.02	08.83	<b>27.23</b>	08.35	12.62	08.23	15.80	15.22	08.27	07.23	11.88
GCH <sub>IC</sub>	15.19	18.48	<b>17.36</b>	10.22	22.79	10.84	22.87	11.31	11.63	11.59	15.23
CCV	06.93	10.66	<b>29.52</b>	09.67	16.23	07.16	15.68	14.27	08.97	08.32	12.74
CCV <sub>IC</sub>	16.16	20.51	<b>18.46</b>	10.19	24.66	11.29	23.45	12.66	11.92	13.57	16.29
BIC	07.38	09.88	<b>28.91</b>	10.26	16.17	07.58	16.56	<b>15.33</b>	08.80	08.45	12.93
BIC <sub>IC</sub>	15.79	19.84	<b>18.14</b>	10.51	23.94	11.48	23.52	<b>11.54</b>	11.68	13.96	16.04
CDH	10.90	19.81	18.85	10.85	12.68	07.48	10.45	14.12	08.34	12.95	12.64
CDH <sub>IC</sub>	17.08	26.23	20.53	14.89	25.38	11.80	24.25	19.82	12.38	20.00	19.24
SEH	15.70	18.93	<b>28.92</b>	12.70	<b>18.31</b>	<b>12.25</b>	<b>25.81</b>	16.80	11.10	<b>14.99</b>	17.55
SEH <sub>IC</sub>	19.29	20.69	<b>26.74</b>	14.03	<b>17.90</b>	<b>12.08</b>	<b>25.47</b>	17.89	11.11	<b>13.57</b>	17.88
SSLBP	14.23	23.27	<b>26.18</b>	<b>13.63</b>	<b>23.39</b>	<b>13.87</b>	18.67	16.57	09.60	12.20	17.16
SSLCP <sub>IC</sub>	15.51	25.27	<b>16.82</b>	<b>12.50</b>	<b>20.67</b>	<b>11.19</b>	25.66	19.76	10.31	17.51	17.52

The RAP and RAR values are not improved by most of the features for dragon category because the area of dragon in the images is less (i.e. background features are dominated over the foreground features). In these Tables, the highlighted ones are the results that are not improvement and most of them are reported for dragon category, but still the overall results are still better using proposed method as depicted by the OAP and OAR values of Table 4 and Table 5 respectively. Fig. 16(b-m) shows the top 10 images retrieved by each features to a query image of type elephant displayed in Fig. 16(a) from Corel-non-uniform dataset using d<sub>CDH</sub> distance. It should be noted that, there are total 100 similar images to the query image in the dataset among which 5 images are the just different instances of the query image with varying degree of non-uniform illumination difference. The retrieval precision achieved using each GCH, CCV and BIC features are just 20% whereas it is 90%, 100% and 100% for GCH<sub>IC</sub>, CCV<sub>IC</sub> and BIC<sub>IC</sub> (see Fig. 16(b-g)). CCV<sub>IC</sub> and BIC<sub>IC</sub> are able to retrieve all instances of the query image while 4 instances are retrieved using GCH<sub>IC</sub>. Both CDH and CDH<sub>IC</sub> obtained 70% precision by retrieving 7 images of the elephant category but only two instances of query image is returned using CDH whereas all five instances are returned by the CDH<sub>IC</sub> (Fig. 16(h-i)). Nearly same situation also depicted in Fig. 16(j-k) for the case of SEH and SEH<sub>IC</sub> where both gained 50% precision but SEH retrieved 4 instances while SEH<sub>IC</sub> retrieved all five instances. Similar scenario also arises with SSLBP and SSLBP<sub>IC</sub> where for both system

returned 8 similar images but the output images using  $SSLBP_{IC}$  are more semantically accurate by retrieving all instances of query image at different non-uniform illumination. In the case of Corel-non-uniform dataset, all the features in proposed illumination compensated color space are more robust and perform better.

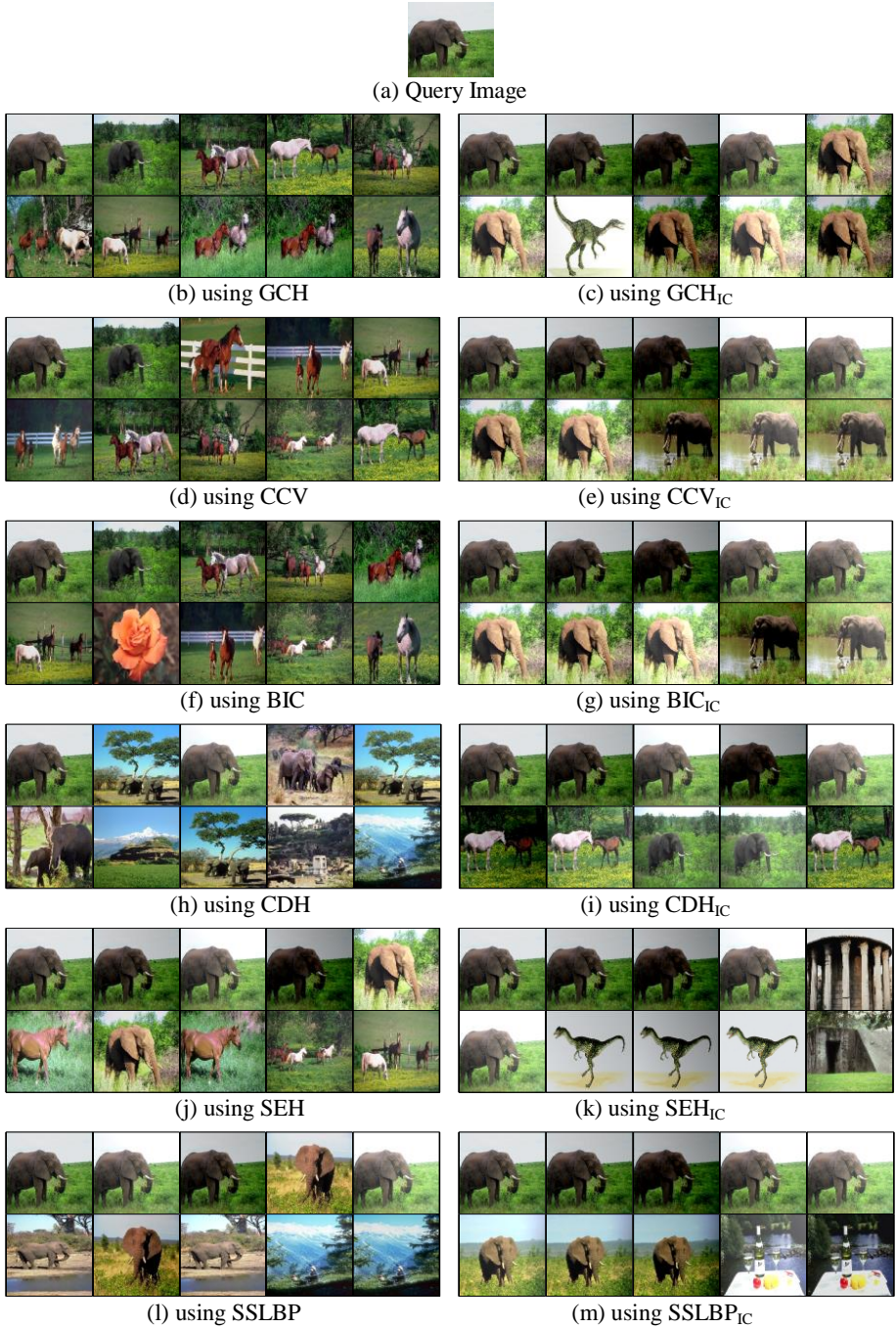


Fig. 16 Image retrieval results overt Corel-non-uniform dataset using  $d_{CDH}$  distance.

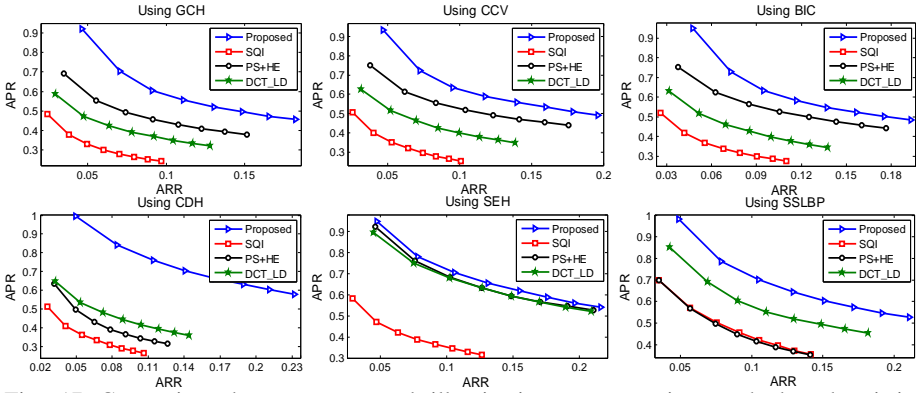


Fig. 17 Comparison between proposed illumination compensation method and existing illumination compensation methods in terms of the retrieval performance over Corel-non-uniform dataset using GCH, CCV, BIC, CDH, SEH and SSLBP feature descriptors.

## 5.4 Comparison and Analysis

In this section, first we compare the proposed illumination compensation method with existing illumination compensation methods, then we test the efficiency of the proposed approach using illumination invariant descriptors, then we analyze the performance of proposed approach by changing the linear function to logarithmic function used in the contrast mapping, and finally in the last, we analyze the limiting change in the illumination allowed over which introduced method can be applied effectively.

### 5.4.1 Comparison with existing illumination compensation methods

To demonstrate the efficiency and discriminative ability of proposed illumination compensation mechanism using color intensity reduction and contrast mapping, we compared its performance with the performance of existing illumination compensation mechanisms such as self-quotient image (SQI) [37, 25], plane subtraction and histogram equalization (PS+HE) [33, 24] and discrete cosine transform in logarithmic domain ( $DCT_{LD}$ ) [3]. Figure 17 illustrates the precision-recall curve by applying GCH, CCV, BIC, CDH, SEH and SSLBP feature descriptors with proposed, SQI, PS+HE and  $DCT_{LD}$  illumination compensation methods over Corel-non-uniform dataset using  $d_{CDH}$  distance measure. The performance of proposed method is too much improved with the CDH descriptor because our method is based on the color information and CHD is also based on the color information. From the experimental results, it is clear that the proposed approach outperforms the existing approaches for illumination invariant image retrieval task in terms of the APR and ARR values.

### 5.4.2 Performance evaluation using illumination invariant descriptors

We also tested our approach with illumination invariant descriptors such as local binary pattern (LBP) [18], centre symmetric local binary pattern (CSLBP) [13], local intensity order pattern (LIOP) [7], local ternary pattern (LTP) [34], centre symmetric local ternary pattern (CSLTP) [12] and histogram of oriented gradients (HOG) [4] because these descriptors already care about the illumination.

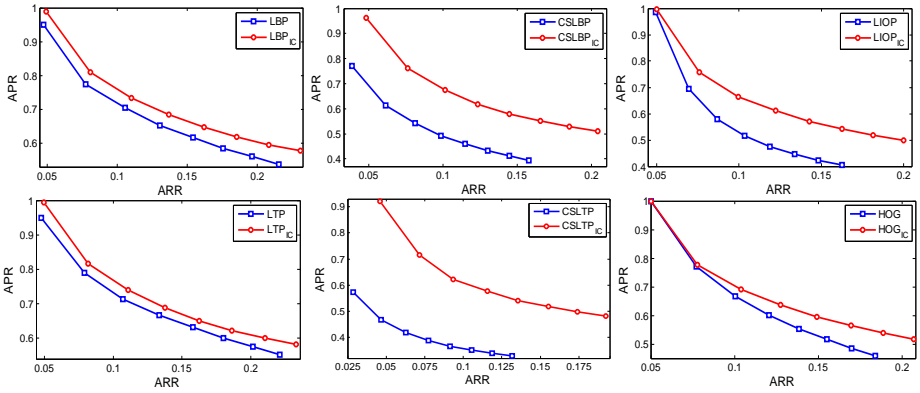


Fig. 18 Performance evaluation of proposed illumination compensation approach using illumination invariant feature descriptors LBP, CSLBP, LIOP, LTP, CSLTP and HOG over Corel-non-uniform dataset.

Figure 18 presents the precision-recall plot over Corel-non-uniform dataset using different illumination invariant descriptor with and without our illumination compensation step using  $d_{CDH}$  distance measure. We observed across the plots that the performance of each illumination invariant descriptor is improved significantly in conjunction with our illumination reduction step as compared to the without using our method. It concludes that although some descriptors are illumination invariant in nature but can't handle the complex illumination difference which required an efficient illumination compensation mechanism. It is also observed that the feature descriptors with low dimension such as CSLBP and CSLTP are having more improvement as compared to the feature descriptors with high dimension.

### 5.4.3 Analysis over contrast mapping

We have used a linear function in the contrast mapping step of the proposed illumination compensation mechanism. In this section, we reported the results using logarithmic function for contrast mapping and compared it with the results of the linear function.

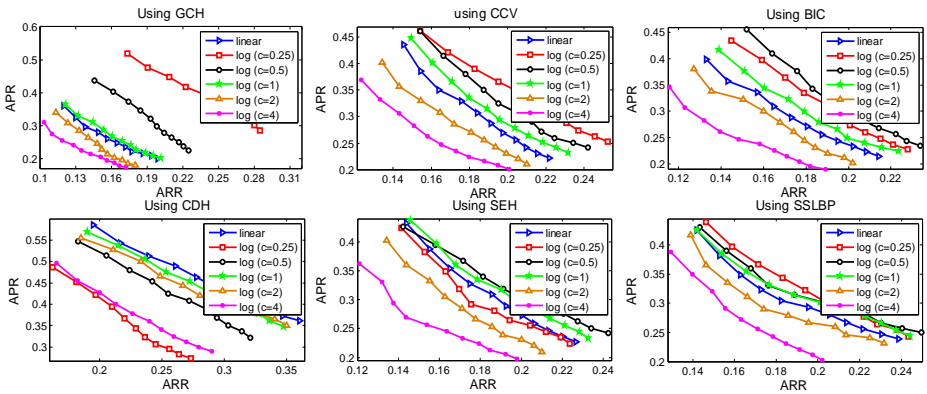


Fig. 19 Comparison of performances among different contrast mapping functions over Phos dataset using GCH, CCV, BIC, CDH, SEH and SSLBP feature descriptors.



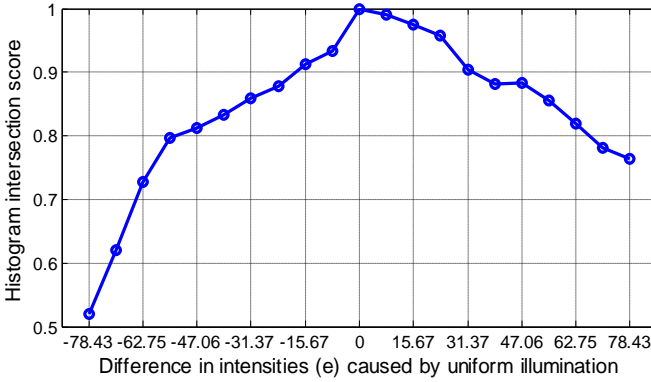


Fig. 20 Effect of intensity difference (e) in % caused by the change in illumination over histogram intersection score.

The logarithmic function is defined as,

$$I' = c \times \log(1 + I) \tag{26}$$

where  $I$  is the input image,  $\log$  is the logarithmic operator,  $c$  is a constant and  $I'$  is the output image.

We experimented with the different values of  $c$  such as 0.25, 0.5, 1, 2 and 4 in this paper and compared their performances. Figure 19 presents the precision-recall curve using different feature descriptors for different functions of contrast mapping over Phos dataset using  $d_{CDH}$  distance measure. It is deduced across the plots that the performance of logarithmic function is better than the performance of linear function using most of the feature descriptors only if the value of parameter  $c$  in (27) is greater than or equal to 1 (i.e.  $c \geq 1$ ). Otherwise, the linear mapping is better choice than logarithmic mapping (i.e.  $c < 1$ ). Specially, the retrieval performance using GCH feature is gained too much with the higher value of  $c$  of logarithmic contrast mapping.

#### 5.4.4 Analysis over limiting change in illumination

We have performed an experiment to find the limiting values of the intensity change (e) caused by the uniform illumination difference. We collected to 20 random images from the corel-dataset and generated the images by considering  $e$  (used in Equation (4)) from -78.43% to +78.43%. All the images generated are then transformed into the  $R_{IC}G_{IC}B_{IC}$  color space according to the proposed method. We applied the histogram intersection method to compute the similarity among the histograms of original image with the histograms of generated images in  $R_{IC}G_{IC}B_{IC}$  color space. Finally we considered the average for each 20 images selected initially. The histogram intersection score (HIS) between two histograms  $FD$  and  $TD$  of dimension  $dim$  is calculated as,

$$HIS = \frac{\sum_{dim} \min(FD, TD)}{\sum_{dim} FD} \tag{27}$$

where ‘ $min$ ’ is the operator to find the minimum of each bin from two vectors. The high value of HIS indicates the high similarity of the image and vice-versa. The average HIS is reported in the Figure 20 for with different value of  $e$ (%). It can be seen that for exactly same images HIS is 1 and if we consider that more than 90% of HIS is representing high similarity then the limiting value of  $e$  will be from -15.67% to 31.37%.

## 6 Conclusion

An illumination invariant color space transformation is presented in this paper. The new illumination compensated color space  $R_{IC}G_{IC}B_{IC}$  is generated by first removing the intensity information from the R, G and B channels of RGB image and after by contrast stretching. Introduced multi-channel based illumination compensation mechanism can be seen as a pre-processing step to remove the effect of illumination variations over the image. Proposed approach is generic and can be used with most of the color feature descriptors but applicable only to those scenarios where illumination robust image matching is required. We tested the performance in image retrieval problem using 6 state-of-the-art features over 3 datasets having images with varying illuminations including standard Phos illumination benchmark. The proposed approach outperforms the existing illumination compensation approaches. The performances of illumination invariant feature descriptors are also boosted in conjunction with the proposed illumination compensation mechanism. The experimental results point out the robustness of the proposed mechanism and suggest that it can be successfully utilized as a pre-processing to compensate the effect of illumination.

## References

1. Andreou I, Sgouros NM (2007) Utilizing shape retrieval in sketch synthesis. *Multimedia Tools and Applications* 32(3):275-291
2. Chen HH, Ding JJ, Sheu HT (2013) Image retrieval based on quadtree classified vector quantization. *Multimedia Tools and Applications*, pp 1-24
3. Chen W, Er MJ, Wu S (2006) Illumination compensation and normalization for robust face recognition using discrete cosine transform in logarithm domain. *IEEE transactions on systems, man, and cybernetics. Part B, Cybernetics* 36: 458–466
4. Dalal N, Triggs B (2005) Histograms of oriented gradients for human detection. In: *IEEE Computer Society Conference on Computer Vision and Pattern Recognition*, pp. 886-893
5. Daoudi I, Idrissi K (2014) A fast and efficient fuzzy approximation-based indexing for CBIR. *Multimedia Tools and Applications*, pp 1-27
6. Dubey SR, Jalal AS (2012) Detection and Classification of Apple Fruit Diseases Using Complete Local Binary Patterns. In *3<sup>rd</sup> IEEE International Conference on Computer and Communication Technology (IC CCT)*, pp. 346-351
7. Fan B, Wu F (2011) Local Intensity Order Pattern for feature description. In: *International Conference on Computer Vision*, pp 603–610
8. Gevrekci M, Gunturk BK (2009) Illumination robust interest point detection. *Computer Vision and Image Understanding*, 113(4):565–571
9. Gonzalez RC, Woods RE (2007) *Digital Image Processing (3rd Edition)*. Prentice Hall
10. Guo Z, Zhang D (2010) A completed modeling of local binary pattern operator for texture classification. *IEEE Transactions on Image Processing* 19(6):1657-1663
11. Gupta R, Mittal A (2008) SMD : A Locally Stable Monotonic Change Invariant Feature Descriptor. In: *Computer Vision–ECCV*, pp 265-277
12. Gupta R, Patil H, Mittal A (2010) Robust order-based methods for feature description. In: *IEEE Conference on Computer Vision and Pattern Recognition (CVPR)*, pp 334–341
13. Heikkilä M, Pietikäinen M, Schmid C (2009) Description of interest regions with local binary patterns. *Pattern Recognition*, 42(3):425–436
14. Hernández-Gracidas CA, Sucar LE, Montes-y-Gómez M (2013) Improving image retrieval by using spatial relations. *Multimedia Tools and Applications* 62(2):479-505
15. Hu R, Jia W, Ling H, Zhao Y, Gui J (2014) Angular Pattern and Binary Angular Pattern for Shape Retrieval. *IEEE Transactions on Image Processing* 23(3):1118-1127
16. Irtaza A, Jaffar MA, Aleisa E, Choi TS (2013) Embedding neural networks for semantic association in content based image retrieval. *Multimedia Tools and Applications*, pp 1-21
17. Liu G-H, Yang J-Y (2013) Content-based image retrieval using color difference histogram. *Pattern Recognition* 46(1):188–198

18. Member S, Ma T (2002) Multiresolution Gray-Scale and Rotation Invariant Texture Classification with Local Binary Patterns. *IEEE Transactions on Image Processing* 24(7):971–987
19. Moreno-noguer F, De Rob I (2010) Deformation and Illumination Invariant Feature Point Descriptor. In: *IEEE Conference on Computer Vision and Pattern Recognition (CVPR)*, pp 1593-1600
20. Murala S, Maheshwari RP, Balasubramanian R (2012) Local tetra patterns: a new feature descriptor for content-based image retrieval. *IEEE Transactions on Image Processing* 21(5):2874–2886
21. Pass G, Zabih R, Miller J (1997) Comparing images using color coherence vectors. In: *4th ACM international conference on Multimedia*, pp 65-73
22. Ranganathan A, Matsumoto S, Ilstrup D (2013) Towards illumination invariance for visual localization. In: *IEEE International Conference on Robotics and Automation (ICRA)*, pp 3791 – 3798
23. Rashedi E, Nezamabadi-pour H, Saryazdi S (2013) Information fusion between short term learning and long term learning in content based image retrieval systems. *Multimedia Tools and Applications*, pp 1-24
24. Ruiz-del-Solar J, Navarrete P (2005) Eigenspace-based face recognition: a comparative study of different approaches. *IEEE Transactions on Systems, Man, and Cybernetics, Part C: Applications and Reviews* 35(3):315-325
25. Ruiz-del-Solar J, Quinteros J (2008) Illumination compensation and normalization in eigenspace-based face recognition: A comparative study of different pre-processing approaches. *Pattern Recognition Letters* 29(14):1966-1979
26. Saavedra JM, Bustos B (2013) Sketch-based image retrieval using keyshapes. *Multimedia Tools and Applications*, pp 1-30
27. Saipullah KM, Kim DH (2012) A robust texture feature extraction using the localized angular phase. *Multimedia Tools and Applications* 59(3):717-747
28. Shahabi C, Safar M (2007) An experimental study of alternative shape-based image retrieval techniques. *Multimedia Tools and Applications* 32(1):29-48
29. Shamsi A, Nezamabadi-pour H, Saryazdi S (2013) A short-term learning approach based on similarity refinement in content-based image retrieval. *Multimedia Tools and Applications*, pp 1-15
30. Shi Z, Liu X, Li Q, He Q, Shi Z (2012) Extracting discriminative features for CBIR. *Multimedia Tools and Applications* 61(2):263-279
31. Singh N, Dubey SR, Dixit P, Gupta JP (2012) Semantic Image Retrieval by Combining Color, Texture and Shape Features. In: *International Conference on Computing Sciences (ICCS)*, pp. 116-120
32. Stehling RO, Nascimento MA, Falcão AX (2002) A compact and efficient image retrieval approach based on border/interior pixel classification. In: *11th international conference on Information and knowledge management*, pp 102-109
33. Sung KK, Poggio T (1998) Example-based learning for view-based human face detection. *IEEE Transactions on Pattern Analysis and Machine Intelligence* 20(1):39-51
34. Tan X, Triggs B (2010) Enhanced local texture feature sets for face recognition under difficult lighting conditions. *IEEE Transactions on Image Processing* 19(6):1635-1650
35. Tang F, Lim SH, Chang NL, Alto P (2009) A Novel Feature Descriptor Invariant to Complex Brightness Changes. In: *IEEE Conference on Computer Vision and Pattern Recognition (CVPR)*, pp 2631–2638
36. Vacha P, Haindl M (2007) Image retrieval measures based on illumination invariant textural MRF features. In: *6<sup>th</sup> ACM international conference on Image and video retrieval*, pp 448-454
37. Wang H, Li SZ, Wang Y (2004) Face recognition under varying lighting conditions using self quotient image. In: *Sixth IEEE International Conference on Automatic Face and Gesture Recognition*, pp. 819-824
38. Wang S, Zheng J, Hu H-M, Li B (2013) Naturalness preserved enhancement algorithm for non-uniform illumination images. *IEEE Transactions on Image Processing* 22(9):3538–3548
39. Wang X, Wang Z (2013) A novel method for image retrieval based on structure elements' descriptor. *Journal of Visual Communication and Image Representation*, 24(1):63–74
40. Wang XY, Wu JF, Yang HY (2009) Robust image retrieval based on color histogram of local feature regions. *Multimedia Tools and Applications* 49(2):323–345
41. Wang XY, Zhang BB, Yang HY (2012) Content-based image retrieval by integrating color and texture features. *Multimedia Tools and Applications*, pp 1-25
42. Wang Z, Liu G, Yang Y (2012) A new ROI based image retrieval system using an auxiliary Gaussian weighting scheme. *Multimedia Tools and Applications*, pp 1-21
43. Wu J, Shen H, Li YD, Xiao ZB, Lu MY, Wang CL (2013) Learning a Hybrid Similarity Measure for Image Retrieval. *Pattern Recognition* 46(11):2927-2939
44. Zhu J (2013) Logarithm Gradient Histogram : A General Illumination Invariant Descriptor for Face Recognition. In: *10<sup>th</sup> IEEE International Conference and Workshops on Automatic Face and Gesture Recognition (FG)*, pp 1-8